Published in final edited form as:
Circ Res. 2012 March 30; 110(7): 990–999. doi:10.1161/CIRCRESAHA.112.264440.

Explaining Calcium-Dependent Gating of Anoctamin-1 Chloride Channels Requires a Revised Topology

Kuai Yu, **Charity Duran**, **Zhiqiang Qu**, **Yuan-Yuan Cui**, and **H. Criss Hartzell**
Department of Cell Biology, Emory University School of Medicine

Abstract

Rationale—Ca^{2+}-activated Cl channels (CaCCs) play pivotal roles in the cardiovascular system: they regulate vascular smooth muscle tone and participate in cardiac action potential repolarization in some species. CaCCs were recently discovered to be encoded by members of the Anoctamin (Ano, also called Tmem16) superfamily, but the mechanisms of Ano1 gating by Ca^{2+} remain enigmatic.

Objective—The objective was to identify regions of Ano1 involved in channel gating by Ca^{2+}.

Methods and results—The Ca^{2+} sensitivity of Ano1 was estimated from rates of current activation and deactivation in excised patches rapidly switched between zero and high Ca^{2+} on the cytoplasmic side. Mutation of glutamates E702 and E705 dramatically altered Ca^{2+} sensitivity. E702 and E705 are predicted to be in an extracellular loop, but antigenic epitopes introduced into this loop are not accessible to extracellular antibodies, suggesting this loop is intracellular. Cytoplasmically-applied membrane-impermeant sulfhydryl reagents alter the Ca^{2+} sensitivity of Ano1 E702C and E705C, as expected if E702 and E705 are intracellular. Substituted cysteine accessibility mutagenesis of the putative re-entrant loop suggests that E702 and E705 are located adjacent to the Cl conduction pathway.

Conclusions—We propose an alternative model of Ano1 topology based on mutagenesis, epitope accessibility, and cysteine-scanning accessibility. These data contradict the popular re-entrant loop model by showing that the putative 4th extracellular loop (ECL 4) is intracellular and may contain a Ca^{2+} binding site. These studies provide new perspectives on regulation of Ano1 by Ca^{2+}.

Keywords

chloride channel; calcium; ion channel; patch clamp; transmembrane topology

Introduction

Calcium-activated chloride channels (CaCCs) play vital roles in the cardiovascular system [1–4]. In vascular smooth muscle, vasoconstrictor-stimulated mobilization of Ca^{2+} from intracellular stores opens CaCCs that serve in a positive feedback loop to sustain contraction by depolarizing the membrane and activating Ca^{2+} influx through voltage-gated Ca^{2+} channels. In portal vein smooth muscle, Ca^{2+} sparks generated from ryanodine-sensitive stores can activate CaCCs to generate spontaneous transient inward currents, which depolarize and activate voltage-gated Ca^{2+} channels. In cardiac myocytes of some species,

Corresponding Author: H. Criss Hartzell, Address: Department of Cell Biology, Emory University School of Medicine, 615 Michael St., Atlanta, GA 30322, Fax: 404-727-6256, Tel: 404-242-5719, criss.hartzell@emory.edu.

Disclosures
The authors state that they have no conflict of interest.

including rabbit, pig, dog, and sheep, but probably not human, CaCC currents have been shown to play a role in cardiac action potential repolarization and to participate in arrhythmogenesis [5, 6]. Recently, it has been proposed that the health benefits (including reduced risk of cardiovascular disease) of red wine and green tea may be explained by the direct effects of gallotannins on CaCCs [7].

Although the cardiovascular significance of CaCCs has long been apparent, understanding how these channels operate has been slow to develop because the molecular identity of CaCCs was not discovered until 2008, when three labs identified Tmem16A, now known as Ano1, as an essential subunit of CaCCs [8–10]. Ano1 is a member of a 10-gene superfamily, of which two members, Ano1 and Ano2, have been clearly shown to encode CaCCs that participate in fluid and salt transport by epithelia, slow wave activity in the gut, regulation of smooth muscle contraction, and control of cellular excitability [11–13]. Ano1 has been shown to encode CaCCs in vascular smooth muscles [14–16].

Understanding how Ano1 channels operate requires knowledge of how Ca^{2+} causes the channel to open. Even before CaCCs were identified at the molecular level, it was noticed that the biophyscial properties of CaCC currents depend on Ca^{2+} concentration: submicromolar Ca^{2+} activates a current that strongly outwardly rectifies and is time-dependent, whereas higher concentrations activate an instantaneous current with no rectification. This difference is physiologically relevant because it determines, for example, whether epithelial CaCCs function in a secretory or absorptive capacity or neuronal CaCCs carry outward or inward current [17, 18]. However, it is enigmatic how voltage- and Ca^{2+}-dependent gating comes about molecularly, largely because the location of the Ca^{2+} binding site(s) and the anion-selective pore remain unknown.

Studies on the structure-function of Ano1 to date have been guided by a topology model of eight transmembrane α-helices with a re-entrant loop between transmembrane helices 5 and 6. This model is based on hydropathy analysis [19] and experiments performed on Ano7 [20]. However, the validity of this model for Ano1 has not been experimentally established. This is especially critical because Ano7 has not yet been shown to be a Cl channel and because the amino acid sequences of Ano1 and Ano7 are only 32% identical [11, 21]. The putative re-entrant loop has been a prime suspect for the channel pore in Ano1 because the R621E mutation was reported to drastically alter the anion-to-cation selectivity of the channel [8]. Experiments described below raised questions in our mind about the location of the pore and stimulated us to re-examine the topology of Ano1 and potential Ca^{2+} binding sites. Our revised model moves the previously-designated 4th extracellular loop to an intracellular location and identifies a potential Ca^{2+}-binding site in this domain. This model has the attractive feature that it places a Ca^{2+} binding site immediately adjacent to the pore and provides insights into Ano1 channel gating.

Materials and Methods

Methods have previously been described [18] and are presented in detail in the online supplement. The mAno1 **a, c** splice variant (Accession: Q8BHY3) was used. Mutations were made using PCR-based mutagenesis. mAno1 was transfected into HEK293 cells using Fugene-6; (Roche Molecular Biochemicals, Indianapolis, IN). Transfected HEK293 cells were patch clamped using conventional whole-cell and excised inside-out patches. The zero Ca^{2+} intracellular solution contained (mmol/L): 146 CsCl, 2 $MgCl_2$, 5 EGTA, 10 HEPES, 10 sucrose, pH 7.3, adjusted with NMDG. High Ca^{2+} pipette solution contained 5 mmol/L Ca^{2+}-EGTA, instead of EGTA (free Ca^{2+} 20 μM). The 126 μM and 2 mmol/L Ca^{2+} were made by adding 0.2 mmol/L and 2 mmol/L $CaCl_2$ to high-Ca^{2+} solution. The standard extracellular solution contained (mmol/L): 140 NaCl, 5 KCl, 2 $CaCl_2$, 1 $MgCl_2$, 15 glucose,

10 HEPES, pH 7.4 with NaOH. Relative anion permeability was determined by measuring the shift in zero-current E_{rev} after changing the bath solution from 151 mmol/L Cl^- to 140 mmol/L substitute anion (X^-) plus 11 mmol/L Cl^-. The permeability (P) ratio was calculated by using the Goldman-Hodgkin-Katz equation. Permeability of Na^+ or Cs^+ relative to Cl^- was determined by measuring changes in zero-current E_{rev} when the concentration of extracellular NaCl or CsCl was changed ("dilution potential" method). The fast application of Ca^{2+} to excised inside-out patches was performed using a double-barreled theta tubing with a tip diameter of ~50 μm attached to a piezobimorph on a micromanipulator. One barrel was filled with standard zero-$[Ca^{2+}]_i$ solution, and the other barrel was filled with intracellular solution containing the indicated free Ca^{2+}. The time course of solution exchange across the laminar flow interface was estimated by liquid junction potential measurements to be 0.5 ms (10–90% rise time) for a 10-fold difference in ionic strength. mAno1 with inserted human influenza hemaglutinin (HA) epitopes at various positions were used to determine the topology by assessing the accessibility of the HA epitope to extracellularly applied antibody. Cells were fixed for 15 min at room temperature in 1% paraformaldehyde in 0.1mol/L phosphate buffer pH 7. Non-permeabilized cells were washed in 3 times in blocking buffer. Permeabilized cells were incubated in blocking buffer containing 0.15% - 0.3% Triton-X100. Cells were incubated with anti-HA antibody diluted 1:750 in blocking buffer for 2 h at room temperature, washed 3 times in blocking buffer, and then incubated in goat-anti-rabbit IgG conjugated with Dylight-549 (Jackson Immunochemicals).

Results

Topology of mAno1

We used 14 different web servers employing different strategies to predict mAno1 transmembrane domains (Online Table I). All algorithms consistently identified 7 segments corresponding to TMDs 1–4 and 6–8 in Fig. 1B (left panel). Two algorithms failed to identify TMD5 and five algorithms identified the proposed re-entrant loop as a TMD. In light of this ambiguity, we wanted to clarify Ano1 topology. We introduced HA epitopes into mAno1-EGFP at various positions (570, 614, 672, 700, or 824, Fig. 1A), expressed the constructs in HEK cells, and then evaluated the accessibility of the introduced epitopes to extracellularly-applied antibodies in permeabilized and non-permeabilized cells by confocal microscopy. We first performed patch clamp recording to verify that the introduction of the epitope did not destroy channel function. All of the constructs exhibited currents characteristic of Ano1 (Fig. 1A, right table) and mAno1-EGFP fluorescence at the membrane (Fig. 1A, left panels) indicating that the HA insertions did not significantly alter the tertiary structure of the channel. In non-permeabilized cells, HA epitopes were accessible to extracellular anti-HA antibody only at positions 614 and 824 (Fig. 1A, middle panels); all the other positions were inaccessible. The inaccessibility of the epitopes introduced at 672 and 700 is not consistent with the topology shown in Fig. 1B (left panel) and suggests that the putative extracellular loop 4 (amino acids 650 – 706) is oriented intracellularly.

E702 and E705 contribute to Ca^{2+} Gating

This revised Ano1 topology suggests new possibilities for the mechanism of channel gating by Ca^{2+}. Amino acids 650–706, which were previously thought to form an extracellular loop, contain a sequence that is highly conserved among all members of the Anoctamin superfamily: [E/D]-[Y/F]-[M/L/Q]-E-[M/T/L/Q]. In Ano1 and Ano2, this sequence is invariably $_{702}$EYMEM. To test whether this region is involved in channel function, E702 and E705 in mAno1 were replaced with glutamines. This double mutation exhibited an apparent reduction in Ca^{2+} sensitivity (Fig. 2). The E702Q/E705Q mutant was activated

only a small amount by 20 μM Ca^{2+}, a concentration that maximally activated WT Ano1, but E702Q/E705Q was significantly activated by 100-fold higher Ca^{2+} concentrations (2mM Ca^{2+}). This concentration of Ca^{2+} had no effect on Cl^- currents in untransfected HEK cells (Online Fig. I).

We have previously shown that Ano1 can be activated by high voltage in the absence of Ca^{2+} [18]. High-voltage-activated currents for E702Q/E705Q and WT were similar in amplitude (WT: 46.1 ± 10.4 pA/pF, n=10; E702Q/E705Q: 45.0 ± 7.6 pA/pF, n=5 at +200 mV; p = 0.66), supporting the suggestion that this mutation mainly affects Ca^{2+}-dependent gating while having little effect on voltage-dependent gating. Furthermore, the current activated by 500 μM Ca^{2+} was very strongly outwardly rectifying, which is characteristic of WT Ano1 currents that are activated by sub-maximal [Ca^{2+}]. Voltage-dependent activation and deactivation of the current were accelerated, as expected if the apparent affinity of the channel for Ca^{2+} were decreased [18].

We then examined the effects of mutation of E702 and E705 individually. The conservative E702D substitution produced currents that were similar to WT but with slightly more outward rectification. In contrast, the charge-reversal E702K dramatically decreased Ca^{2+}-activated current (Fig. 2E). Both the conservative E705D and the charge-reversal E705K mutations exhibited markedly reduced Ca^{2+}-dependent activation (Fig. 2E). These results suggest that both E702 and E705 are important in Ca^{2+} sensing or gating.

To quantify the effects of E702 and E705 substitutions on Ca^{2+}-dependent gating, we performed experiments in which inside-out excised patches were rapidly switched between zero and high Ca^{2+} within several ms [18] (Fig. 3). Current decay was well-fit by a monoexponential equation. The time constant of deactivation (τ_{off}), was V_m-dependent and was greatly accelerated by the E702Q and E705Q mutations (Fig. 3E). At +120 mV, τ_{off} was 408.4 ± 67.3 ms for WT, 40.4 ± 4.1 ms for E702Q, and 96.3 ± 6.6 ms for E705Q.

In principle, the process of current deactivation upon switching to zero Ca^{2+} involves two steps: Ca^{2+} dissociation from its binding site followed by channel closure. However, the process is very likely dominated by Ca^{2+} dissociation because τ_{off} is strongly dependent upon the ligand (Ba^{2+} or Ca^{2+}) used to activate the channel [18] (see Discussion).

The time constant of activation (τ_{on}) of Ano1 current upon switching to Ca^{2+}-containing solutions is dependent on [Ca^{2+}], as expected if Ca^{2+} binding is a rate-limiting step in channel activation [17, 18]. At +120 mV with 82 μmol/L [Ca^{2+}], τ_{on} for WT current was 5.1 ± 1.1 ms, but was ~25-times slower for E705Q, 131.1 ± 20.2 ms (Fig. 3D). At very high [Ca^{2+}] of 2 mM, τ_{on} for E705Q was still slower than wild type (35.9 ± 7.8 ms). The E702Q mutation had a smaller effect on τ_{on} than the E705Q mutation (Fig. 3D). τ_{on} of E702Q was indistinguishable from WT at 82 μmol/L Ca^{2+}, but under these conditions τ_{on} is close to the switching time of the perfusion system and therefore not quantitatively reliable. However, lower Ca^{2+} concentrations could not be tested for E702Q because the current amplitude with low [Ca^{2+}] was too small for accurate measurement.

The very slow τ_{on} observed with E705Q raised questions in our minds about possible artifacts of the fast perfusion system. To test the validity of this approach, we measured the activation of currents in response to photolysis of caged Ca^{2+} (NP-EGTA) under whole cell patch clamp. For the same intensity UV flash, WT currents activated much more quickly than E705Q currents (Online Fig. II). At the same flash intensity (90 mJ), E705Q activated with a time constant (τ_{on} = 80 msec) that was >20-times slower than WT (τ_{on} = 3.7 msec) (Online Fig. I). These values are somewhat faster than those observed with rapid perfusion using 82 μmol/L Ca^{2+} because the [Ca^{2+}] released by photolysis was presumably greater

than this. Activation of E702Q was consistently >20-times slower than WT at all equivalent flash intensities.

Assuming that the predominant rate-limiting steps in Ano1 current activation and deactivation in these experiments are Ca^{2+} binding and unbinding, the apparent EC_{50} for Ca^{2+} can be calculated as $EC_{50} = \alpha/\beta$, where $\alpha = 1/\tau_{off}$ and $\beta = \{(1/\tau_{on})-\alpha\}/[Ca^{2+}]$. The calculations were performed with data utilizing different Ca^{2+} concentrations that provided reliable on-rates for wild type and mutant channels. The E705Q mutation increases the EC_{50} at all voltages (Fig. 3F), suggesting that it plays a key role in Ca^{2+} sensing. The EC_{50} for E702Q is likely underestimated as noted above.

Thiol reagents alter Ca^{2+} sensitivity of E702C and E705C

Alteration of the Ca^{2+} sensitivity of mAno1 by changing the charge at E702 and E705 by mutagenesis is consistent with the hypothesis that these amino acids contribute to a Ca^{2+} binding site. To test this hypothesis using a different approach, we asked whether modification of thiols introduced at these positions by charged MTS reagents would also alter Ca^{2+} sensitivity. E702 or E705 were replaced with cysteine and the effects of charged thiol reagents, $MTSET^+$ and $MTSES^-$, on channel gating by Ca^{2+} were measured in fast perfusion experiments. The MTS reagents were applied to the cytoplasmic face of inside-out excised patches. mAno1 has at least 5 cysteines that are predicted to be cytoplasmic, but neither $MTSET^+$ nor $MTSES^-$ had any significant effect on the amplitude or kinetics of activation or deactivation of wild type mAno1 when applied to the cytoplasmic face of the patch (Fig. 4C–E). E702C (unmodified by MTS reagent) was much less sensitive to Ca^{2+} than wild type mAno1. At +120 mV, the EC_{50} for E702C was 114 μmol/L, compared to 0.94 μmol/L for WT and 21 μmol/L for E702Q. The larger EC_{50} for E702C compared to E702Q might be explained if the side chain oxygen of glutamine participates in Ca^{2+} coordination. $MTSET^+$ increased the EC_{50} of E702C ~30-fold (from 114 μmol/L to ~ 3 mmol/L at 120 mV) by slowing τ_{on} and accelerating τ_{off} (Fig. 4F–H). The decrease in Ca^{2+} affinity was accompanied by a decrease in current amplitude (56.4 ± 10.8%), as expected. $MTSES^-$ had the opposite effect on EC_{50} (Fig. 4F–H) and the uncharged MTSEH had no effect (Online Fig. IIIA). At 0 mV, the EC_{50}'s were estimated to be 550 μmol/L for unmodified E702C, ~3890 μmol/L (extrapolated) for $MTSET^+$-modified, and 144 μmol/L for $MTSES^-$-modified currents. The results with E705C exhibited a similar trend but were decidedly less dramatic, possibly because of reduced accessibility of MTS reagents to this residue which is surrounded by very hydrophobic amino acids.

If E702 and E705 are located on the cytoplasmic side of the membrane, we would predict that MTS reagents applied from the extracellular side would have no effect on E702C or E705C currents. We tested this prediction using whole-cell recording because outside-out patches could be obtained with only very low success. We also tested several other cysteine-substituted amino acids nearby. In whole-cell recording, extracellular application of $MTSET^+$ and $MTSES^-$ had no significant effect on E702C or E705C currents ($MTSET^+$ increased E702C currents by 4.7 ± 6.6 % and decreased E705C by −3.1 ± 0.9 %). This compares to a decrease of 56.4 ± 10.8% for E702C in excised patches exposed to cytosolic $MTSET^+$. $MTSET^+$ had no significant effect on any of the currents generated by these cysteine-substituted mutants (Online Fig. IIIB).

Online Fig. IV shows the time courses of the current changes caused by cytoplasmic MTS reagents on E702C and WT in inside-out excised patches. Currents were activated by a low concentration of Ca^{2+} in order to maximize the change in current amplitude that was produced by a change in Ca^{2+} affinity. $MTSET^+$ (1 mmol/L) decreased the current with a τ = 52 msec and a rate constant of $\sim 2\times10^4\ M^{-1}s^{-1}$. This rate is close to the rate of modification of mercaptoethanol by $MTSET^+$ in solution ($\sim 10^5\ M^{-1}s^{-1}$), suggesting that

these residues are freely accessible to the aqueous environment. The effect of $MTSES^-$ is slower than $MTSET^+$, but because $MTSES^-$ reacts with mercaptoethanol in solution about 5-times slower than $MTSET^-$, this result is also consistent with high aqueous accessibility.

Cysteine accessibility to probe residues near the pore

The region between F620 and N650 has been proposed to be important in forming the Ano1 pore because mutagenesis of positively charged amino acids (notably R621) in this region were reported to drastically alter ion selectivity [8]. The R621E mutant was reported to exhibit a P_{Na}/P_K ratio of 0.87 compared to 0.03 for wild type. We have tried without success to confirm these observations using several different methods. In Fig. 5, P_{Na}/P_{Cl} and P_{Cs}/P_{Cl} were determined by the dilution potential method [22]. The ionic selectivity was found to be identical for WT (P_{Na}/P_{Cl} = 0.13; P_{Cs}/P_{Cl} = 0.08) and R621E (P_{Na}/P_{Cl} = 0.14; P_{Cs}/P_{Cl} = 0.1). The lack of effect of the R621E mutation on ion selectivity raised questions in our mind whether the pore of Ano1 was indeed located in this region.

We used substituted cysteine accessibility mutagenesis [23] to glean more information about the topology of the putative re-entrant loop. mAno1 has 16 native cysteines which could possibly compromise the interpretation of the effects of thiol reagents on introduced cysteines. To determine which endogenous cysteines might be essential for Ano1 function, we first synthesized a cysteine-less mAno1 where all cysteines were replaced with serines. The cysteine-less mutant trafficked to the plasma membrane, as judged by the presence of a bright ring of fluorescence of the mAno1-EGFP tag at the cell surface, but it did not generate currents. To determine which cysteines were important for function, a series of mutants were generated with individual cysteines or groups of cysteines replaced with serine (Online Table II). Six cysteines (C370, C379, C383, C386, C395, or C836) were essential for Ano1 current. The essential cysteines are predicted to be extracellular: five are located in the first extracellular loop and one is located in the last extracellular loop. An Ano1 construct having the six essential cysteines intact and the remaining ten cysteines substituted with serine ($mAno1_{6C}$: C23S/C49S/C166S/C259S/C357S/C559S/C625S/C630S/C635S/C933S) exhibited identical biophysical properties to the wild type channel but had a reduced current amplitude. Replacing any one of the remaining six cysteines (C370, C379, C383, C386, C395, or C836) with serine in $Ano1_{6C}$ completely eliminated the current (Fig. 6A). Because these six cysteines were essential for mAno1 function, the $mAno1_{6C}$ construct was used as the template for cysteine scanning mutagenesis. Extracellular $MTSET^+$, $MTSES^-$, or $MTSEA^+$ had little effect on $Ano1_{6C}$ (Fig. 6C).

Each amino acid from F620 to Q646 in $mAno1_{6C}$ was replaced with cysteine and extracellular MTS reagents were tested in whole cell recording (an example is shown in Fig. 6B). Cysteine substitution at positions 620–629, 633–634, and 637–638 significantly reduced current amplitude (Fig. 6C). $MTSET^+$ significantly stimulated G628C, G629C and $S630C^*$ currents, while $MTSES^-$ decreased $S625C^*$, G628C and M632C currents (Fig. 6D). (The asterisk denotes that this position is a native cysteine in wild type mAno1, but is mutated from S to C in $mAno1_{6C}$). These results support the idea that this region is important in channel function.

To locate amino acids that might be deeper in the pore, we tested the effect of $MTSEA^+$, which is more membrane permeant than $MTSET^+$ [24]. $MTSEA^+$ significantly increased I636C and Q637C currents, suggesting that these amino acids are located deeper in the membrane. In addition, $MTSET^+$ increased K645C current extremely slowly over ~10 min (this is not reflected in summary data because the increase was so slow). Although our analysis cannot formally distinguish between a re-entrant loop and a membrane-spanning segment, these data are consistent with amino acids 625–630 contributing to an outer vestibule that is easily accessible to the extracellular fluid and amino acids beyond 635

being located deep in the pore. To determine whether these amino acids are located in the permeation pathway, we measured the relative iodide permeability (P_I/P_{Cl}) and conductance (G_I/G_{Cl}) of the cysteine-substituted mAno1$_{6C}$ with the expectation that amino acids in the permeation pathway might affect ionic selectivity. However, none of the mutations significantly altered the ionic selectivity (Fig. 7). We also measured the relative Na^+ permeability and conductance of selected mutants and did not detect any significant differences. These data suggest that this region of the protein may contribute to the permeation pathway but is not critical for forming the selectivity filter.

Discussion

The Ca^{2+} sensor of Ano1

One contender for the Ca^{2+} binding site is a stretch of 5 glutamic acids located in the first intracellular loop because of its resemblance to the “Ca-bowl” of the large-conductance K channel [18]. Although a naturally-occurring splice variant (Δ_{448}EAVK$_{451}$) that deletes the 5th glutamic acid increases the EC_{50} for Ca^{2+} ~50-fold, neutralization of the first 4 glutamic acids ($_{444}$EEEE$_{447}$ changed to alanines) has little effect on Ca^{2+} sensitivity [18]. Because Δ_{448}EAVK$_{451}$ and $_{444}$EEEE/AAAA$_{447}$ also alter the voltage-dependent gating of the channel in the absence of Ca^{2+}, we have suggested that the penta-glutamate region couples Ca^{2+} and voltage to channel opening, but is unlikely to be a major Ca^{2+} binding site itself. Other studies have implicated sites in the N-terminus as possible Ca^{2+} or CaM binding sites [25, 26], but there remains no consensus about the mechanisms of Ca^{2+} regulation.

The data presented here strongly implicate another region in Ca^{2+}regulation. Surprisingly, this region was predicted to be an extracellular loop from hydropathy analysis and by analogy to Ano7, another member of the anoctamin superfamily [20]. However, there is no convincing evidence that Ano7 is a Cl^- channel. In our hands, Ano7 does not traffic to the plasma membrane or generate currents in transfected cells and is largely intracellular in adult human prostate where it is normally expressed [21]. In a study by Schreiber et al. [27] it was suggested that Ano7 might function as a CaCC. However, in iodide flux assays, the ATP-stimulated flux in Ano7-transfected cells was similar to untransfected cells and <10% as large as in Ano1-transfected cells. The ionomycin-stimulated iodide flux in Ano7-transfected cells was actually less than in untransfected cells. Furthermore, the short form of Ano7 (Ano7S), which is a 179 amino acid protein with no predicted transmembrane domains, produced approximately the same iodide flux as the long form of Ano7. This supports the idea that Ano7 is not a plasma membrane CaCC and raises the possibility that the topology of Ano7 is different than that of Ano1.

A revised topology is required to explain our data

Our data show that HA tags introduced at positions 672 and 700 in Ano1 are not accessible to extracellular antibody. Furthermore, when E702 and E705 are replaced with cysteine, exposure of the cytosolic face of the membrane to membrane-impermeant MTS reagents causes a rapid change in current amplitude and/or Ca^{2+} sensitivity. This provides an independent piece of data that these residues are intracellular and not extracellular.

If this region is indeed intracellular, a transmembrane segment must exist somewhere between positions 614 where the introduced HA epitope is extracellular and 672 where the HA epitope is intracellular. Although computer algorithms for predicting transmembrane domains do not consistently identify a transmembrane domain between amino acids 614 and 672, between positions 631 and 648, 12 of the 18 amino acids are hydrophobic. Based on secondary structure predictions, all but one of the hydrophilic amino acids are located on one face of this segment. On this basis, we believe that residues 631–648 may form a

transmembrane segment. The problem with this model is that the HA epitope introduced at position 824 is clearly extracellular, which means that there must be an even number of transmembrane segments between 614 and 824. Attempts to probe the topology of this region were unsuccessful because introduction of HA epitopes at several positions in this region produced channels that were non-functional or poorly expressed.

The first four and last two transmembrane segments of mAno1 are consistently identified by transmembrane prediction algorithms. These segments all exhibit a characteristic feature: tryptophan and basic residues are located at the predicted membrane interfaces. This is a common feature of transmembrane segments: tryptophan has a strong preference for lipid carbonyls and the hydrophobic aspects of the long side chains of lysine and arginine interact with the hydrophobic core of the membrane [28]. However, in contrast to the six transmembrane segments that exhibit these characteristic features, the two putative transmembrane segments located between them lack these features. This suggests that the central part of the protein may have a more complex topology than previously predicted. A similar uncertainty existed regarding the transmembrane topology of the ClC transporters before they were crystallized [29]. The uncertainty stemmed from the fact that the ClC transmembrane α-helices are variable in length and tilted at different angles relative to the plane of the membrane. Understanding the organization of mAno1 further will likely have to await direct structural studies.

Effects of thiol reagents support an intracellular location of E702 and E705

One observation that we believe strongly supports the hypothesis that E702 and E705 are intracellular is the finding that altering the charge on E702C and E705C with membrane-impermeant charged MTS reagents changes the Ca^{2+} affinity of the channel. $MTSET^{+}$ renders the channel less sensitive to Ca^{2+} activation whereas $MTSES^{-}$ shifts the Ca^{2+} sensitivity of the channel closer to that of wild type. The size and charge of $MTSES^{-}$-modified cysteine makes it an excellent surrogate for glutamic acid because $MTSES^{-}$-modified cysteine is almost exactly the same volume as glutamic acid (142 $Å^3$ for $MTSES^{-}$-modified cysteine compared to 138 $Å^3$ for glutamic acid) and the negative charge is relatively localized with an estimated charge of −0.79 on each oxygen (a preferred Ca^{2+} ligand) on the sulfonatoethyl group [30]. In contrast, $MTSET^{+}$ is larger (~173$Å^3$) and its charge density is relatively diffuse. The +1 charge on $MTSET^{-}$ is distributed over ~17 atoms. This explains why addition of positive charge by cysteine modification by $MTSET^{+}$ does not itself activate the channel, because its charge density is low compared to Ca^{2+}, which has a +2 charge in a volume of ~20 $Å^3$.

Separation of effects on Ca^{2+} binding and channel gating

Channel gating by Ca^{2+} involves at least 2 steps: Ca^{2+} binding and channel opening/closing. Because these steps are allosterically coupled, it is very difficult to unambiguously separate the effect of a mutation on Ca^{2+} binding from channel gating. However, we believe that the effects of the E702 and E705 mutations on the activation and deactivation of Ano1in response to Ca^{2+} jumps are most simply interpreted in terms of changes in Ca^{2+} binding. We have shown that the rates of Ano1 activation and deactivation depend upon the ligand used [18]. For example, channel deactivation is more rapid and activation is slower using Ba^{2+} as ligand compared to Ca^{2+}. The simplest explanation of these data is that ligand binding and unbinding are the predominant rate-limiting steps and that the probability of the channel being open in the absence of bound ligand is negligible. It is hard to imagine a mechanism that would change the open time that is dependent on the species of ligand (Ca, Ba) but is independent of ligand dissociation. Although one could argue that Ba^{2+} and Ca^{2+} place the channel into different conformations that relax with different kinetics upon ligand dissociation, there is no precedent supporting such an hypothesis.

Physiological significance of Ca^{2+} gating of Ano1

CaCCs participate in the transient outward current (I_{to}) that plays a role in repolarization of the action potential in some species. The best-studied component of I_{to} is a K^+ current mediated by $K_V4.x/K_V1.4$ channels, but in some species, CaCC currents comprise a significant fraction of I_{to} [31]. The contribution of CaCC current, because of its dependence on Ca^{2+}, would be expected to increase under conditions of Ca^{2+} overload and could lead to arrhythmogenesis. CaCCs have been implicated in T-wave alternans, a prequel to malignant ventricular arrhythmias that occur during left ventricular hypertrophy [32], and delayed afterdepolarizations that may lead to arrhythmias [33, 34]. Drugs targeting Ano1 could potentially provide new therapies for hypertension and/or cardiac arrhythmias.

Elucidating the molecular mechanisms of Ano1 gating is essential for developing new therapies targeting these channels. High-throughput screens have identified small molecule inhibitors and activators of Ano1 [7, 35–38]. However, evaluating these drugs requires a molecular understanding of how the Ano1 channel is gated. For example, drugs could activate or inhibit Ano1 channels by altering the affinity of the channel for Ca^{2+} or by affecting how the channel gates open in response to Ca^{2+} or to voltage. Drugs working by these different mechanisms are likely to have different pharmacological effects. For this reason, it is of paramount importance to understand how this channel operates. Another important question is that of possible side-effects of drugs that might occur because Ano1 is ubiquitously expressed in epithelia and smooth muscle of various types. However, Ano1 has multiple splice variants [25, 39], some of which affect the regions that we have identified as important in Ca^{2+} and voltage dependent gating. This not only raises the possibility that variant-specific drugs might be developed, but also emphasizes the importance of structure-function studies to establish the functions of various domains that are drug targets.

Supplementary Material

Refer to Web version on PubMed Central for supplementary material.

Acknowledgments

Sources of funding

Supported by grants from the NIH GM60448 (HCH), EY014852 (HCH), the Microscopy Core of the Emory Neuroscience NINDS Core Facilities Grant P30NS055077, and NEI Core Grant P30EY006360. C. Duran was supported by NEI training grant 5T32EY007092-25.

Non-standard abbreviations and acronyms

Ano1	anoctamin-1, Tmem16a
CaCC	calcium-activated chloride channel
HA	human influenza hemaglutinin
MTSET	[2-Trimethylammonioethyl]-methanethiosulfonate bromide
MTSES	sodium [2-sulfonatoethyl]-methanethiosulfonate
MTSEA	[2-aminoethyl]-methanethiosulfonate hydrobromide
TMD	transmembrane domain

References

1. Leblanc N, Ledoux J, Saleh S, Sanguinetti A, Angermann J, O'Driscoll K, Britton F, Perrino BA, Greenwood IA. Regulation of calcium-activated chloride channels in smooth muscle cells: A complex picture is emerging. Can J Physiol Pharmacol. 2005; 83:541–556. [PubMed: 16091780]
2. Large WA, Wang Q. Characteristics and physiological role of the Ca^{2+}-activated Cl^{-} conductance in smooth muscle. Am J Physiol. 1996; 271:C435–454. [PubMed: 8769982]
3. Duran C, Thompson CH, Xiao Q, Hartzell HC. Chloride channels: Often enigmatic, rarely predictable. Annu Rev Physiol. 2010; 72:95–121. [PubMed: 19827947]
4. Duan D. Phenomics of cardiac chloride channels: The systematic study of chloride channel function in the heart. J Physiol. 2009; 587:2163–2177. [PubMed: 19171656]
5. Gwanyanya A, Macianskiene R, Bito V, Sipido KR, Vereecke J, Mubagwa K. Inhibition of the calcium-activated chloride current in cardiac ventricular myocytes by n-(p-amylcinnamoyl)anthranilic acid (ACA). Biochemical and Biophysical Research Communications. 2010; 402:531–536. [PubMed: 20971070]
6. Hartzell C, Putzier I, Arreola J. Calcium-activated chloride channels. Annu Rev Physiol. 2005; 67:719–758. [PubMed: 15709976]
7. Namkung W, Thiagarajah JR, Phuan PW, Verkman AS. Inhibition of Ca2+-activated Cl-channels by gallotannins as a possible molecular basis for health benefits of red wine and green tea. FASEB J. 2010; 24:4178–4186. [PubMed: 20581223]
8. Yang YD, Cho H, Koo JY, Tak MH, Cho Y, Shim WS, Park SP, Lee J, Lee B, Kim BM, Raouf R, Shin YK, Oh U. Tmem16A confers receptor-activated calcium-dependent chloride conductance. Nature. 2008; 455:1210–1215. [PubMed: 18724360]
9. Schroeder BC, Cheng T, Jan YN, Jan LY. Expression cloning of Tmem16A as a calcium-activated chloride channel subunit. Cell. 2008; 134:1019–1029. [PubMed: 18805094]
10. Caputo A, Caci E, Ferrera L, Pedemonte N, Barsanti C, Sondo E, Pfeffer U, Ravazzolo R, Zegarra-Moran O, Galietta LJV. Tmem16A, a membrane protein associated with calcium-dependent chloride channel activity. Science. 2008; 322:590–594. [PubMed: 18772398]
11. Duran C, Hartzell HC. Physiological roles and diseases of Tmem16/Anoctamin proteins: Are they all chloride channels? Acta Pharmacol Sin. 2011; 32:685–692. [PubMed: 21642943]
12. Ferrera L, Caputo A, Galietta LJ. Tmem16A protein: A new identity for Ca^{2+}-dependent Cl channels. Physiology (Bethesda). 2010; 25:357–363. [PubMed: 21186280]
13. Kunzelmann K, Tian Y, Martins JR, Faria D, Kongsuphol P, Ousingsawat J, Thevenod F, Roussa E, Rock J, Schreiber R. Anoctamins. Pflugers Arch. 2011; 462:195–208. [PubMed: 21607626]
14. Manoury B, Tamuleviciute A, Tammaro P. Tmem16A/Anoctamin 1 protein mediates calcium-activated chloride currents in pulmonary arterial smooth muscle cells. J Physiol. 2010; 588:2305–2314. [PubMed: 20421283]
15. Davis AJ, Forrest AS, Jepps TA, Valencik ML, Wiwchar M, Singer CA, Sones WR, Greenwood IA, Leblanc N. Expression profile and protein translation of Tmem16A in murine smooth muscle. Am J Physiol Cell Physiol. 2010; 299:C948–959. [PubMed: 20686072]
16. Thomas-Gatewood C, Neeb ZP, Bulley S, Adebiyi A, Bannister JP, Leo MD, Jaggar JH. Tmem16A channels generate Ca^{2+}-activated Cl^{-} currents in cerebral artery smooth muscle cells. Am J Physiol Heart Circ Physiol. 2011
17. Kuruma A, Hartzell HC. Bimodal control of a Ca^{2+} -activated Cl^{-} channel by different ca^{2+} signals. J Gen Physiol. 2000; 115:59–80. [PubMed: 10613919]
18. Xiao Q, Yu K, Perez-Cornejo P, Cui Y, Arreola J, Hartzell HC. Voltage- and calcium-dependent gating of tmem16a/ano1 chloride channels are physically coupled by the first intracellular loop. Proceedings of the National Academy of Sciences. 2011; 108:8891–8896.
19. Milenkovic VM, Brockmann M, Stohr H, Weber BH, Strauss O. Evolution and functional divergence of the anoctamin family of membrane proteins. BMC Evol Biol. 2010; 10:319. [PubMed: 20964844]
20. Das S, Hahn Y, Walker DA, Nagata S, Willingham MC, Peehl DM, Bera TK, Lee B, Pastan I. Topology of NGEP, a prostate-specific cell:Cell junction protein widely expressed in many cancers of different grade level. Cancer Res. 2008; 68:6306–6312. [PubMed: 18676855]

21. Duran C, Qu Z, Osunkoya AO, Cui Y, Hartzell HC. Anos 3–7 in the Anoctamin/Tmem16 Cl^- channel family are intracellular proteins. Am J Physiol Cell Physiol. 2012; 302:C482–493. [PubMed: 22075693]
22. Barry P. The reliability of relative anion-cation permeabilities deduced from reversal (dilution) potential measurements in ion channel studies. Cell Biochemistry and Biophysics. 2006; 46:143–154. [PubMed: 17012755]
23. Karlin A, Akabas MH. Substituted-cysteine accessibility method. Methods in Enzymology. 1998; 293:123–145. [PubMed: 9711606]
24. Holmgren M, Liu Y, Xu Y, Yellen G. On the use of thiol-modifying agents to determine channel topology. Neuropharmacology. 1996; 35:797–804. [PubMed: 8938712]
25. Ferrera L, Caputo A, Ubby I, Bussani E, Zegarra-Moran O, Ravazzolo R, Pagani F, Galietta LJ. Regulation of tmem16a chloride channel properties by alternative splicing. J Biol Chem. 2009; 284:33360–33368. [PubMed: 19819874]
26. Tian Y, Kongsuphol P, Hug M, Ousingsawat J, Witzgall R, Schreiber R, Kunzelmann K. Calmodulin-dependent activation of the epithelial calcium-dependent chloride channel tmem16a. FASEB J. 2010; 25:1058–1068. [PubMed: 21115851]
27. Schreiber R, Uliyakina I, Kongsuphol P, Warth R, Mirza M, Martins JR, Kunzelmann K. Expression and function of epithelial anoctamins. J Biol Chem. 2010; 285:7838–7845. [PubMed: 20056604]
28. Killian JA, von Heijne G. How proteins adapt to a membrane-water interface. Trends Biochem Sci. 2000; 25:429–434. [PubMed: 10973056]
29. Jentsch TJ, Stein V, Weinreich F, Zdebik AA. Molecular structure and physiological function of chloride channels. Physiological Reviews. 2002; 82:503–568. [PubMed: 11917096]
30. Xu Y, Kakhniashvili DA, Gremse DA, Wood DO, Mayor JA, Walters DE, Kaplan RS. The yeast mitochondrial citrate transport protein. Probing the roles of cysteines, arg(181), and arg(189) in transporter function. J Biol Chem. 2000; 275:7117–7124. [PubMed: 10702279]
31. Li GR, Du XL, Siow YL, OK, Tse HF, Lau CP. Calcium-activated transient outward chloride current and phase 1 repolarization of swine ventricular action potential. Cardiovasc Res. 2003; 58:89–98. [PubMed: 12667949]
32. Guo D, Young L, Patel C, Jiao Z, Wu Y, Liu T, Kowey PR, Yan GX. Calcium-activated chloride current contributes to action potential alternations in left ventricular hypertrophy rabbit. Am J Physiol Heart Circ Physiol. 2008; 295:H97–H104. [PubMed: 18441200]
33. Zygmunt AC, Goodrow RJ, Weigel CM. I_{NaCa} and $I_{Cl(Ca)}$ contribute to isoproterenol-induced delayed after depolarizations in midmyocardial cells. American Journal of Physiology. 1998; 275:H1979–H1992. [PubMed: 9843796]
34. Han X, Ferrier GR. Ionic mechanisms of transient inward current in the absence of Na^+-Ca^{2+} exchange in rabbit cardiac purkinje fibres. J Physiol. 1992; 456:19–38. [PubMed: 1284077]
35. Namkung W, Phuan PW, Verkman AS. Tmem16a inhibitors reveal Tmem16a as a minor component of calcium-activated chloride channel conductance in airway and intestinal epithelial cells. J Biol Chem. 2011; 286:2365–2374. [PubMed: 21084298]
36. Namkung W, Yao Z, Finkbeiner WE, Verkman AS. Small-molecule activators of tmem16a, a calcium-activated chloride channel, stimulate epithelial chloride secretion and intestinal contraction. FASEB J. 2011
37. Verkman AS, Galietta LJ. Chloride channels as drug targets. Nat Rev Drug Discov. 2009; 8:153–171. [PubMed: 19153558]
38. De La Fuente R, Namkung W, Mills A, Verkman AS. Small-molecule screen identifies inhibitors of a human intestinal calcium-activated chloride channel. Molecular Pharmacology. 2008; 73:758–768. [PubMed: 18083779]
39. O'Driscoll KE, Pipe RA, Britton FC. Increased complexity of Tmem16a/Anoctamin 1 transcript alternative splicing. BMC Mol Biol. 2011; 12:35. [PubMed: 21824394]

Novelty and Significance

What is known?

- The ion channel Ano1 regulates vascular smooth muscle tone and participates in cardiac action potential repolarization in some species (comprising the current known as I_{to2}).
- Ano1 conducts chloride ions and is activated by increases in intracellular calcium.

What new information does this article contribute?

- The study describes the structural determinants of calcium activation of Ano1.
- The protein domain involved in Ano1 calcium regulation was formerly thought to be extracellular, hence, a new model for the orientation of the channel in the membrane is proposed.
- The study provides insights that may be helpful in designing and evaluating new drugs that target Ano1.

Although chloride channels are known to contribute to cardiovascular regulation, relatively little is known at the molecular level about how they are governed. Here we study how the newly-discovered chloride ion channel Ano1 is turned on by intracellular calcium. We have identified two glutamic acid residues that drastically alter the sensitivity of the channel to intracellular calcium when they are mutated. Surprisingly, these amino acids were previously thought to be located in an extracellular loop. Using a variety of techniques, we suggest that this loop is instead located on the cytoplasmic side of the membrane and is involved in calcium sensing by the channel. These data contradict the popular reentrant loop model by showing that the putative 4th extracellular loop (ECL 4) is intracellular and may contain a Ca^{2+} binding site. Elucidating the molecular mechanisms of Ano1 regulation by calcium is essential for developing new therapies that target these channels. Drugs that target Ano1 could possibly have utility in treating hypertension or arrhythmias.

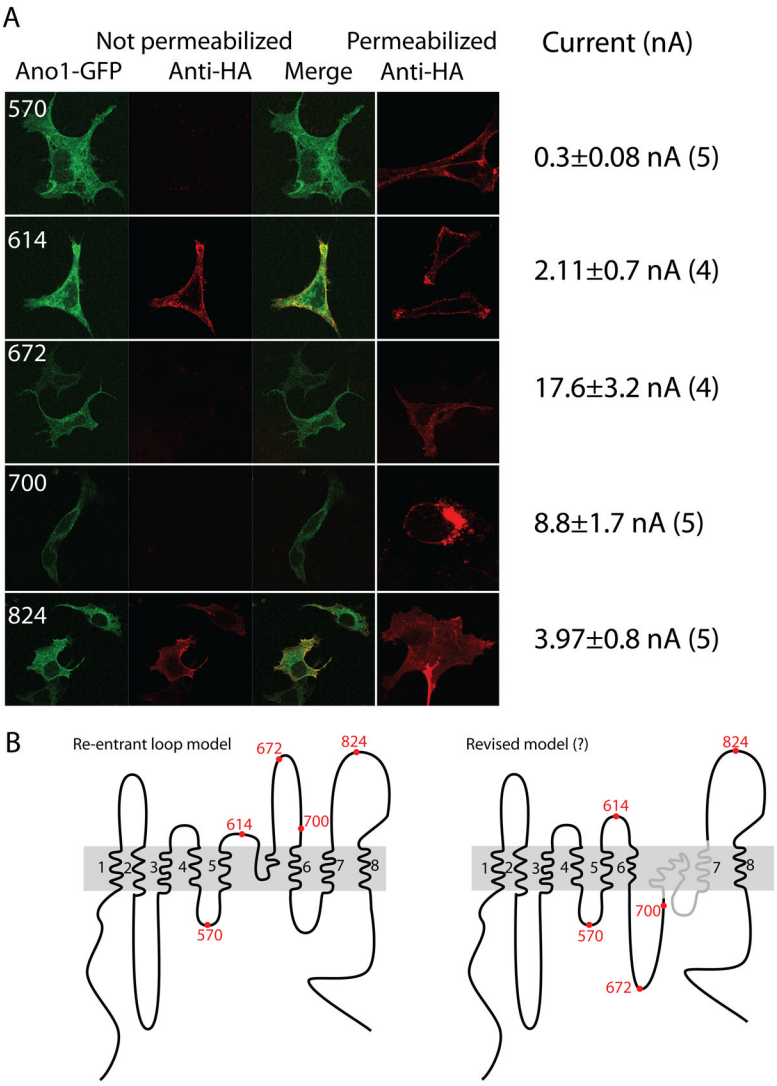

Figure 1.

Immunofluorescent staining of mAno1 containing tandem HA epitopes inserted at various locations. (A) HA tags were inserted into mAno1-EGFP at amino acids 570, 614, 672, 700 and 824. After transient expression, non-permeabilzed intact cells were stained with antibody for HA epitope. Green: Ano1-GFP, Red: Anti-HA, and merged image. Duplicate cover slips were permeabilized prior to incubation with HA antibody (red: permeabilized, anti-HA). For each construct, images were acquired at the same gain and settings, but settings may differ between constructs that were imaged on different days. Raw images from the Zeiss Zen acquisition software from permeabilized and non-permeabilized cells were assembled in Adobe Photoshop CS5 and brightness and contrast adjusted for all 4 panels equally. Ano1 currents for each construct were recorded with 20 μmol/L Ca. Average peak amplitude at +100mV and the number of recorded cells are listed. (B) Topological models of mAno1. The locations of HA tags are indicated with red numbers. Left: re-entrant loop model. Right: revised model. The topology of the sequence depicted in grey remains in question.

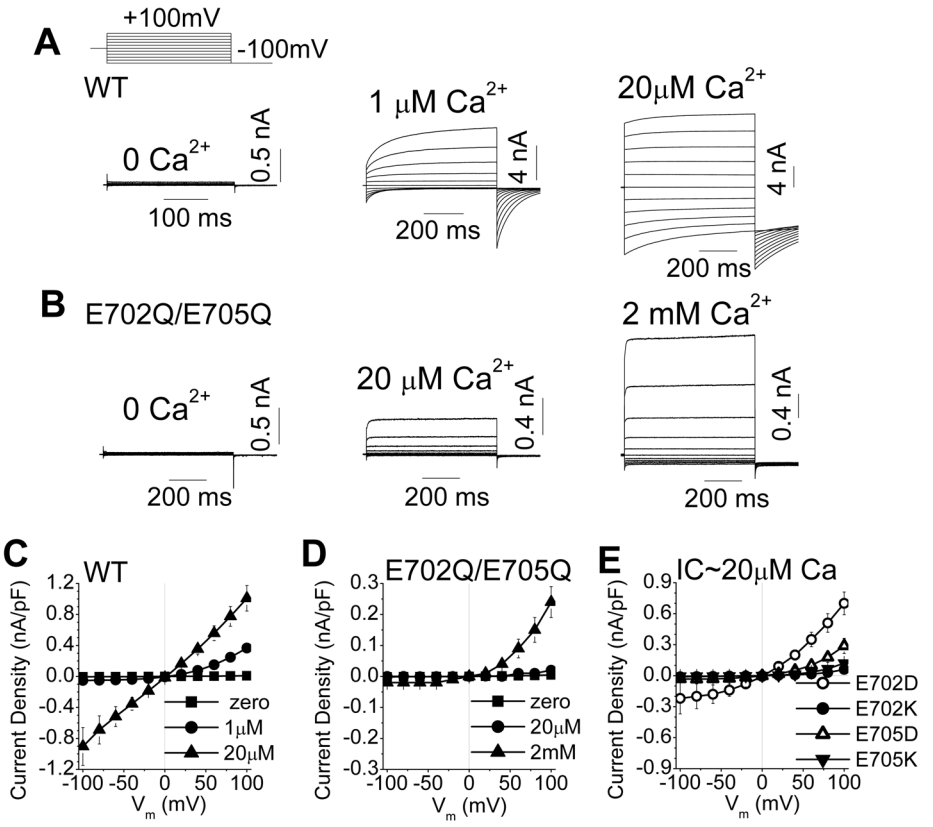

Figure 2.

Mutation of two critical amino acids, E702 and E705, dramatically affects Ca^{2+}-gated but not voltage-gated current of mAno1. (A, B) Representative whole-cell recordings of Ano1 current in transfected HEK293 cells at the indicated free [Ca^{2+}]. Voltage protocol is shown above A. (A) WT-mAno1. (B) E702Q/E705Q mutant mANO1. (C, D) Steady-state current-voltage (I-V) relationships for (C) WT-mAno1and (D) E702Q/E705Q mANO1with different $[Ca]_i$ (N=5–9). (E) I–V relationships for E702D, E702K, E705D and E705K mutants with 20 μmol/L Ca^{2+} (N=5–9).

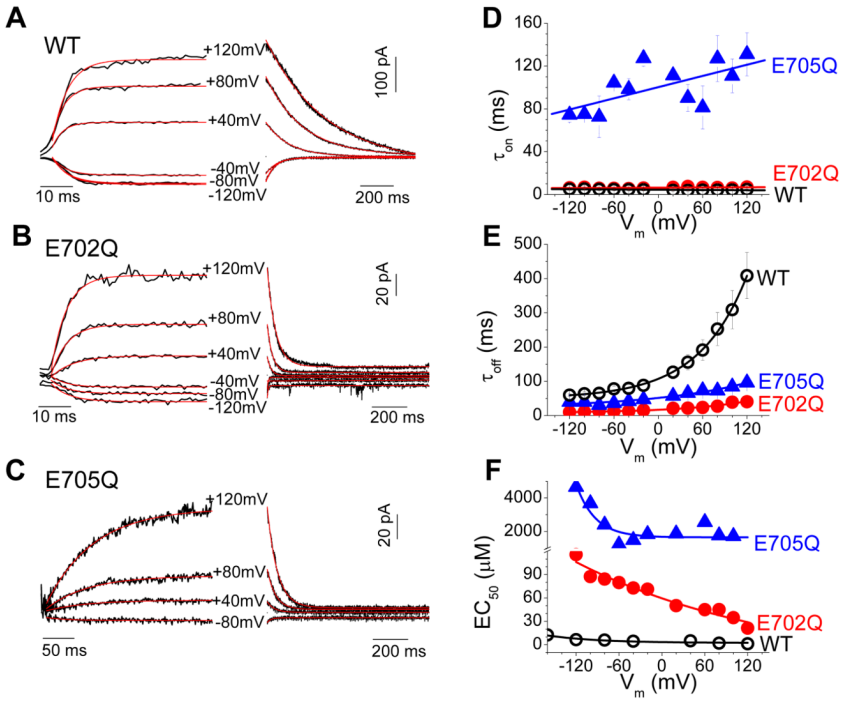

Figure 3.

Activation and deactivation kinetics of Ano1 with rapid Ca^{2+} perfusion in inside-out excised patches. (A–C) Representative traces of Ano1 current in response to application (left) and washout (right) of Ca^{2+} at the indicated holding potentials. (A) WT-mAno1. (B) E702Q mANO1. (C) E705Q mANO1. (D-F) V_m dependence of τ_{on}, τ_{off}, and EC_{50} for WT Ano1 (open circles), E702Q (filled circles), and E705Q (filled triangles).

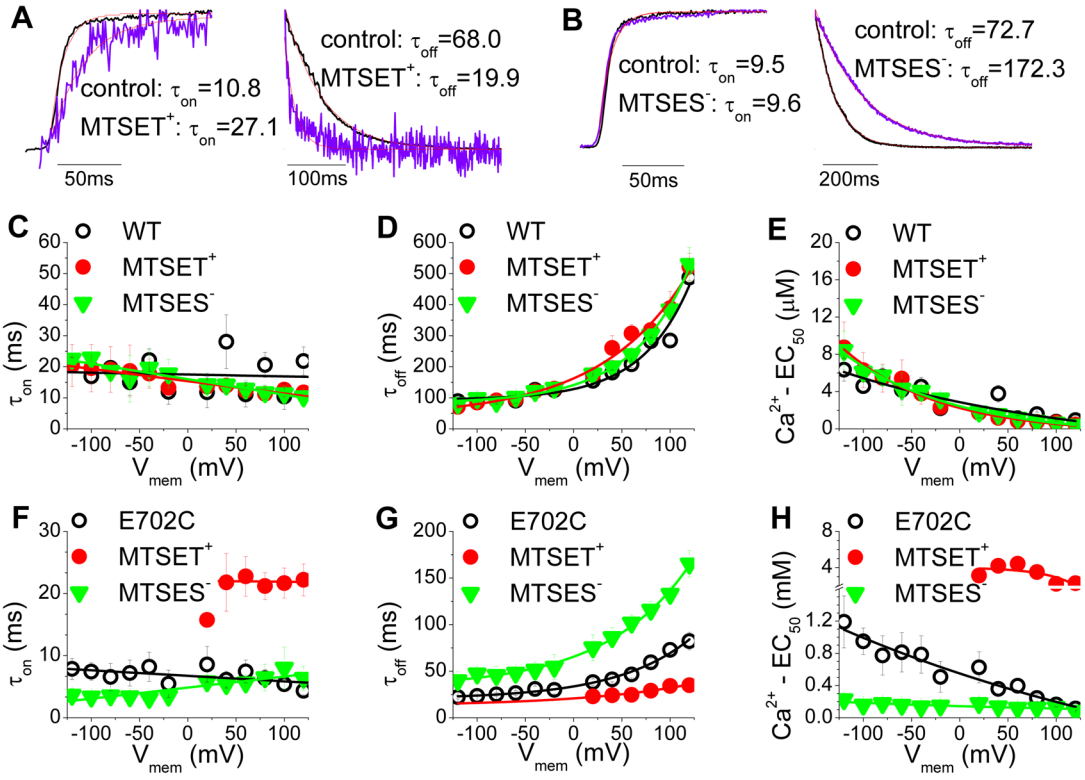

Figure 4.

Effects of sulfhydryl modification on activation and deactivation kinetics of Ano1 in excised inside-out patches with rapid Ca^{2+} perfusion. Excised patches were switched between zero and high Ca^{2+}. They were then exposed to MTS reagent in the presence of zero Ca^{2+} for 10 sec, MTS reagent was washed away, and the patch was switched from zero Ca^{2+} to high Ca^{2+} again. (A, B) Normalized current traces of E702C mAno1showing examples of changes in τ_{on} and τ_{off} caused by $MTSET^+$ (A) and $MTSES^-$ (B). Traces were normalized to the same maximal amplitude. As shown in Fig. S3, $MTSET^+$ causes a decrease in current and $MTSES^-$ increases the current. The magnitude of the effect of MTS reagent on current amplitude depends where on the Ca^{2+}dose-response curve the experiment is performed. (C–E) Lack of effect of MTS reagents on τ_{on}, τ_{off}, and EC_{50} for WT Ano1. (F–H) Effects of MTS reagents on τ_{on}, τ_{off}, and EC_{50} for E702C mAno1. Open circle: before application of MTS reagent. Filled circle: after $MTSET^+$, triangle: after $MTSES^-$. (N=3–6).

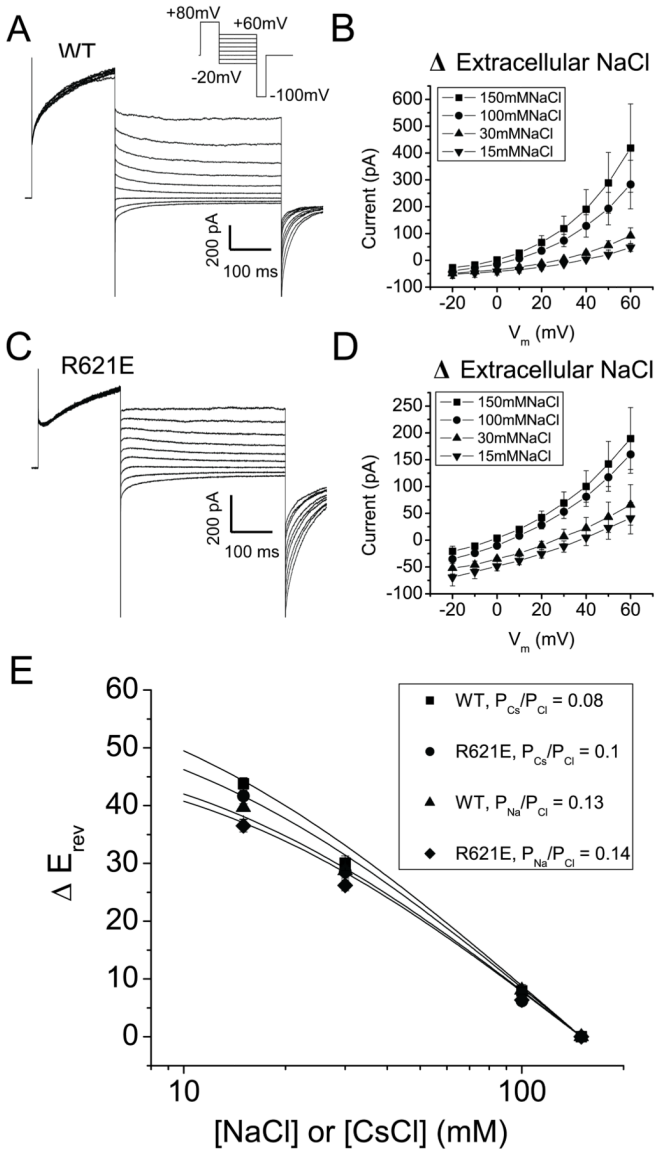

Figure 5.

Effect of R621E mutation on anion:cation permeability of mAno1. (A, B) Whole-cell recordings of (A) WT mAno1 in symmetrical 150 mmol/L NaCl with 180 nmol/L Ca_i and (B) R621E mAno1 in symmetrical 150 mmol/L NaCl with 1.1 μmol/L Ca_i. The R621E mutation decreased the Ca^{2+} sensitivity of the channel, requiring a larger Ca^{2+} concentration to generate a measurable current. (C, D) Current-voltage relationships of (C) WT mAno1 and (D) R621E mAno1 with different extracellular [NaCl]. (E) Change in reversal potential (ΔE_{rev}) for different extracellular [NaCl] or [CsCl] determined from experiments like those in C and D. Lines are best fits to the Goldman-Hodgkin-Katz equation.

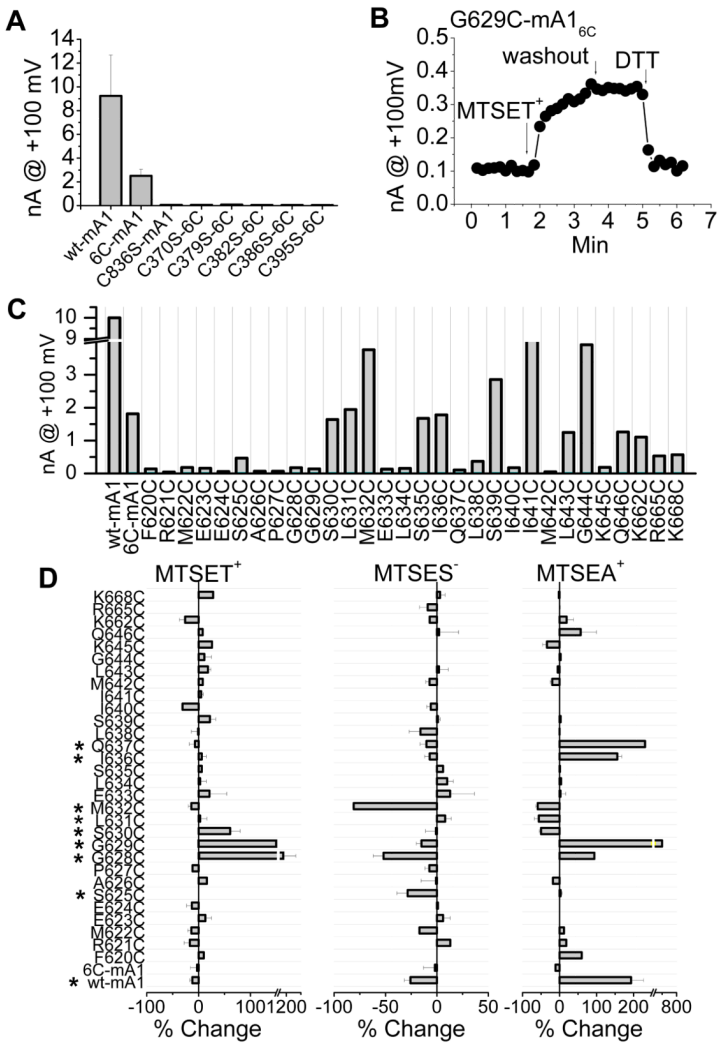

Figure 6.

Essential cysteines in mAno1 and scanning cysteine accessibility of the proposed new TMD6 (amino acids 620–646). (A) Six extracellular cysteines are required for mAno1 function. Amplitudes of whole-cell currents activated by 20μmol/L $[Ca^{2+}]_i$ at +100mV from WT and cysteine-substituted mutants of mAno1 expressed in HEK293 cells. Inset shows location of cysteines (solid red circles: essential; open red circles: not-essential for channel function) in the old model of mAno1. 6C: mAno1 with all cysteines except C370, C379, C383, C386, C395 and C836 replaced with serines. C836S is wild type mAno1 with C836 only replaced with serine. The other constructs have each of the essential cysteines in $mAno1_{6C}$ as indicated replaced with serine. (B) Example of change in current amplitude of G629C $mANO1_{6C}$. MTSET-induced increase in current is not reversed by washout of MTSET but is reversed by 5 mmol/L DTT. (C) Average Ano1 currents recorded from WT mAno1, $mAno1_{6C}$ and cysteine-substituted $mAno1_{6C}$. (D) Effects of $MTSET^+$ (left), $MTSES^-$ (middle) and $MTSEA^+$ (right) on cysteine-substituted $mAno1_{6C}$. The percent change of current at +100mV within 2 min of exposure to MTS reagent was calculated by $[100\ (I_{after\ MTS} - I_{before\ MTS})/I_{before\ MTS}]$. Cysteine-substituted amino acids labeled with an asterisk were significantly ($p < 0.05$) affected by MTS reagents (N= 3–6).

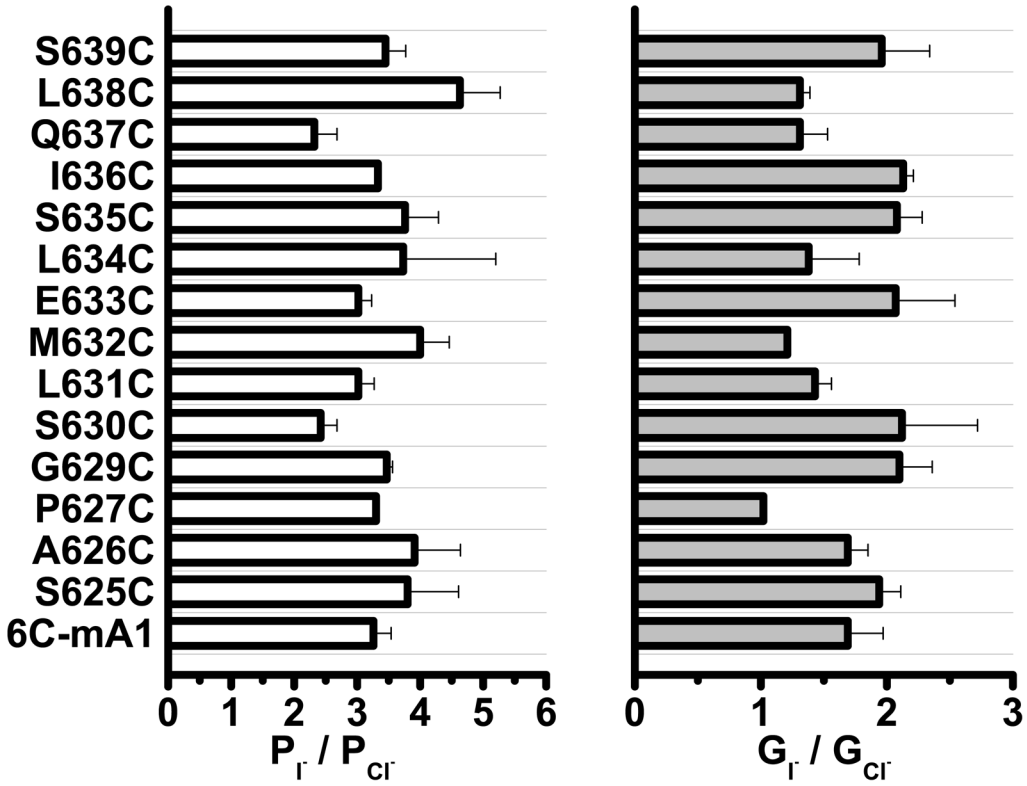

Figure 7.

Effects of replacement of amino acids in $mANO1_{6C}$ with cysteine on I^- permeability and conductance relative to Cl^-. (A) Relative I^- permeability was calculated from the shift in reversal potential after replacing extracellular Cl^- with I^-. (B) Relative I^- conductance was measured as the ratio of slopes of the current-voltage relationship at the reversal potential after and before extracellular anion change (N= 3–10).